Indian Journal of Chemistry
Vol. 63, January 2024, pp. 80-93
DOI: 10.56042/ijc.v63i1.4441

The study of force fields molecular mechanics and molecular quantum on the interaction with drugs of the alkylating agent with SWCNT-BNNT in different solvents and at different temperatures

Mohammad Hassan Jamshidi[a], Neda Hasanzadeh[a], Hooriye Yahyaei*[b] & Amir Bahrami[c]

[a] Department of Chemistry, Ahvaz Branch, Islamic Azad University, Ahvaz, Iran

[b] Department of Chemistry, Zanjan Branch, Islamic Azad University, Zanjan, Iran

[c] Department of Physics, Ahvaz Branch, Islamic Azad University, Ahvaz, Iran

E-mail: hooriye_yahyaei@yahoo.com, mohamadj1362@gmail.com, nhzadeh_212@yahoo.com, bahrami_amir@yahoo.com

Received 29 July 2023; accepted (revised) 21 December 2023

The present study investigates the interaction between two alkylating agent drugs, cyclophosphamide (CP) and mechlorethamine (MC), with Single-Wall carbon nanotubes (SWCNTs) and Boron Nitride nanotubes (BNNTs). Calculations have been performed by using methods of quantum mechanics and molecular mechanics. The effects of different solvents on the interaction of CP and MC with SWCNTs and BNNTs within the Onsager self-consistent reaction field (SCRF) model, as well as the effects of temperature on the stability of the interactions between the compounds in various solvents have been investigated. Thermodynamic parameters, Frontier Molecular Orbitals (FMOs), and Total Density of States (DOS) of the title compounds have been evaluated by using theoretical calculations. Moreover, the interaction of CP and MC with SWCNTs and BNNTs have been examined through AMBER, OPLS, CHARMM, and MM+ force fields through the molecular mechanic (MM) method. The Monte Carlo simulation of CP and MC structures connected to carbon and boron nitride nanotubes in Water, Methanol, Ethanol, DMSO, and Chloroform solvents showed that Chloroform is the most stable solvent for simulation with the lowest energy, which is directly attributed to dielectric constant. Studies show that the results of Monte Carlo, molecular mechanics, and quantum mechanics are consistent with each other in terms of thermodynamic properties and conformer populations.

Keywords: Quantum Monte Carlo (QMC), Single-Wall carbon nanotubes (SWCNTs), Boron Nitride nanotubes (BNNTs), Alkylating agent, Force field

Alkylating agents are highly active compounds, which are capable of forming covalent bonds with the parts of large molecules having the functional group including (OH), (SH), (COOH), amino group, nitrogenous heterosilicate compounds such as nucleic acids, phosphates, amino acids, and proteins. Nitrogen No. 3 and 7 and Oxygen No. 6 in Guanine, nitrogen No. 1, 3, and 7 in Adenine, and nitrogen No. 3 in Cytosine are usually alkylated in nucleic acids. Side effects of the alkylating antineoplastic drugs are related to the creation of alkylation at an improper site of DNA or RNA, which can cause a mistake in copying the information needed to produce proteins, which leads to cell death eventually[1]. The general mechanism of alkylation by alkylating agents is shown in Fig. 1 [2].

Nitrogen mustards were first used for treating Lymphosarcoma in 1942 [3]. Alkylating agents include nitrogen mustards such as mechlorethamine, cyclophosphamide, melphalan, *etc*.[4,5] Reducing the toxic effects of the chemotherapy drugs is one of the goals of pharmacists. Cyclophosphamide is the most effective drug among 1000 compounds evaluated on 33 types of tumours[6,7]. It is the eighth drug, which has FDA-approved anti-cancer and cytotoxic effects. It is activated in the body by the cytochrome P-450 enzyme in the liver and converted to the active metabolites of Phosphoramid mustard and Acrolein[8,9].

Among the studies in the field of nanotechnology and cyclophosphamide, paper[10] can be mentioned, which evaluated the effects of the anti-cancer properties and reducing the side effects of this drug in combination with selenium nanoparticles. In computational research, papers[11] and[12] were recently examined the link between cyclophosphamide and Single-Walled carbon nanotubes.

Although mechlorethamine does not selectively attack the cancer cells, it attacks any fast-growing cell

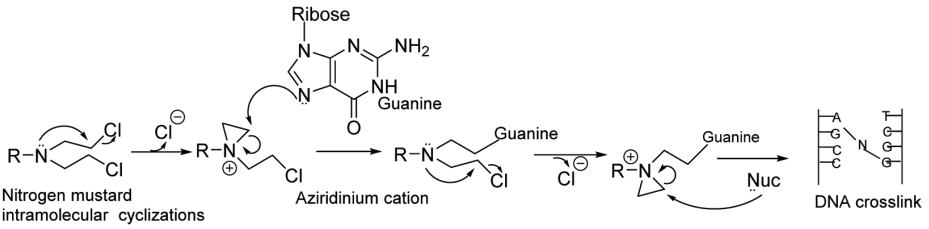

Fig. 1 — General mechanism of alkylation by alkylating agents

such as bone marrow cells[13,14]. Therefore, it can have the side effects such as gene mutation. It is administrated in a drug regimen called MOPP (joncovin-mechlorethamine) for treating Hodgkin's disease. Mechlorethamine were reported to be very effective for the treatment of cutaneous T-cell lymphoma (CTCL) or mycosis fungoides, which is a common example of CTCL. It is highly reactive and unstable, which should be considered in the preparation and formulation of the drug[15]. It becomes an aziridinium ion, which is susceptible to the nucleophilic attack, when dissolved in water. Therefore, it should be used fresh and then discarded[16,17]. Skin allergies is one of the side effects observed in the topical use of this drug[18]. Some studies in the field of computational work[4] were recently performed on the combination of mechlorethamine and fluorine boron nitride nanocarriers. Further, some studies in the field of drug delivery[5] conducted on the lipid nanocarriers and mechlorethamine, which was indicated a reduction in the side effects.

A large number of studies were recently evaluated the drug delivery of single- walled carbon nanotubes. The results of the papers indicated that the bio sensors, which were based on SWCNTS can help in early detection of many cancers[17,19-21]. Boron Nitride Nanotubes (BNNTs) made of boron and nitrogen atoms, discovered in 1995, are structurally identical to carbon nanotubes[22]. The ionic properties of the bond between boron and nitrogen make it chemically resistant to oxidation. BNNTs have a higher temperature tolerance and better solubility compared to CNTS[23,24]. Based on the results of the studies, BNNTs are biocompatible[25], which, can react with polymers or amino molecules for increasing their dissolution property related to the weak π interactions and poor hydrogen bonds[26]. Several studies indicated that boron nanotubes possess the appropriate electron properties[27]. Moreover, BNNTs have high potential for drug delivery due to the nontoxic and bio compatible properties.

Computational Method

The quantum chemical calculations were performed by using the Gaussian 09W software in this stud[28]. The molecular structure of the title compounds was optimized in the ground state by using the Density Functional Theory (DFT/B3LYP/6-31+G*)[29,30]. The Polarized Continuum Model (PCM)[31], Frontier Molecular Orbital (FMO) analysis and electronic properties such as energy of HOMO and LUMO orbitals, HOMO-LUMO energy gap (Eg), ionization potential (I), electron affinity (A), global hardness (η), electronegativity (χ), electronic chemical potential (μ), electrophilicity (ω), and chemical softness (S) were estimated through the EHOMO and ELUMO energies using the B3LYP.6-31+G* level of theory[32-35].

The optimized molecular structures were visualized by using GaussView 05 program[36]. There are three types of QMC including variation, diffusion, and green's functions. These methods act with an openly correlated wave function and calculate the integrals numerically using a Monte Carlo integration. Although these calculations are very time-consuming, they are the most accurate methods known to date. Overall, DFT calculations provide the perfect and increasingly more accurate quantitative results as the molecules under consideration become smaller[37]. DFT methods are accessible in the macro model programs, as well. It is necessary to select a level, which is well-parameterized for the molecular system being investigated. Conformational interconversions are managed by using the precise energy parameters and geometry coordinates, which are vital in the molecular systems too. The Low-energy structures found on each surface were chosen and subjected to the unrestrained quantum mechanical minimization using B3LYP.6-31+G* SCRF[38].

Moreover, the calculations related to the interactions of cyclophosphamide (CP) and mechlorethamine (MC) with Single Wall Carbon Nanotubes (SWCNTs) and Boron Nitride Nanotubes (BNNTs) were performed by using each of the force

fields AMBER[39], OPLS[40], CHARMM[41,42] and MM+ (MM+ is implemented in the molecular modeling package HyperChem)[43] (Fig. 2 and Fig. 3). This method is used in HyperChem software[43]. Four different force fields are available in the Macro Model program. Thus, choosing a force field, which is well parameterized for the molecular system under study, is very important[44].

The Monte Carlo method is one of the most broadly and commonly used numerical techniques, which has applications in statistical physics, quantum mechanics, field theory, *etc*.[45] Monte Carlo simulation, which can generate a canonical ensemble, is used when systems have difficult integrals to be solved and should generate some random numbers to yield statistically fixed and independent values[46,47]. A metropolis algorithm is applied more frequently than other algorithms in the Monte Carlo method due to its simplicity[48]. Random displacement is used for determining the accuracy of the algorithm. Every move can be accepted in minor displacements; however, only a few moves are acceptable in large cases. Differences in force fields are shown in this study by comparing the energies calculated by using the force fields AMBER, OPLS, CHARMM, and MM+. HyperChem professional release 7.01 was used for the Molecular Mechanics calculations. Moreover, Geometry optimization and Monte Carlo simulation were performed by using this software[49].

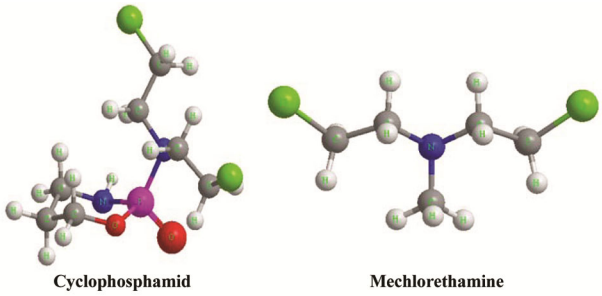

Fig. 2 — Theoretical geometric structure of the cyclophosphamide and mechlorethamine (optimized by B3LYP/6-31+ G* level)

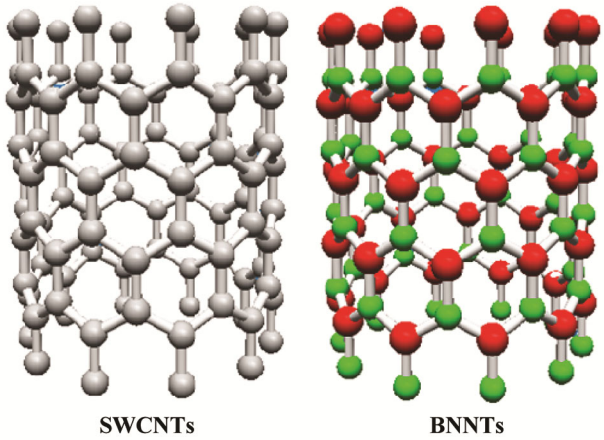

Fig. 3 — Single-Wall Carbon Nanotubes (SWCNTs) and Boron Nitride Nanotubes (BNNTs) (optimized by B3LYP/6-31+G* level)

Results and Discussion

In macromolecules, thermodynamic parameters such as enthalpies, entropies, and free energies depend on many conformational degrees of freedom that these flexible molecules can take. The free energies of macromolecules in solutions cannot typically be estimated using Monte Carlo simulations, partially because transitions from one conformer to another occur infrequently. In addition, Molecular Mechanics simulations regularly succeed in providing more efficient samplings of conformational space in the case of macromolecules. What Monte Carlo or Molecular Dynamics simulations can achieve, however, is estimating free energy differences between similar systems. Such calculations allow, for example, comparison of binding affinities of similar drug molecules with the target receptor, thus facilitating rational design of more potent and selective drugs.

However, a word of caution is needed here. Monte Carlo sampling of the harmonic potentials yields the classical probability distributions, while the bond vibrations are quantized in the real CP and MC atoms with carbon nanotube molecules. Thus, classical Monte Carlo simulations fail to precisely reproduce such thermodynamic properties as heat capacity or vibrational entropy of isolated molecules. Therefore, the quantum mechanics methods were used in this section.

Quantum chemical methods are highly useful tools for acquiring information about the molecular structures and electrochemical behaviors. A Frontier Molecular Orbital (FMO) analysis was performed for the compounds by using the B3LYP/6-311+G (d) level[50]. FMO results such as EHOMO, ELUMO, and the HOMO-LUMO energy gap (ΔE) of the title compounds are given in following tables. Table 1 and Table 2 show the important information related to the quantum mechanics calculations and the stability of CP and MC with SWCNTs and BNNTs. In this step, the CP molecule was first optimized alone and then with SWCNTs and BNNTs.

The energy level of the LUMO and HOMO and their energy gap indicate the chemical reactivity of

Table 1 — Electronic properties of the cyclophosphamide calculated by using the B3LYP/6-31+G* level of theory

Property	CP	CP- SWCNT	CP- BNNT
HF (Hartree)	–1797.557832	–5589.3955307	–9020.7871662
Zero-point correction (Hartree)	0.236439	1.077289	1.570951
Thermal correction to Energy (Hartree)	0.252511	1.137363	1.686926
Thermal correction to Enthalpy (Hartree)	0.253455	1.138307	1.687870
Thermal correction to Gibbs Free Energy (Hartree)	0.189651	1.004015	1.447122
Sum of electronic and zero-point Energies (Hartree)	–1797.321393	–5588.318242	–9019.216216
Sum of electronic and thermal Energies (Hartree)	–1797.305321	–5588.258168	–9019.100241
Sum of electronic and thermal Enthalpies (Hartree)	–1797.304377	–5588.257224	–9019.099296
Sum of electronic and thermal Free Energies (Hartree)	–1797.368181	–5588.391516	–9019.340044
E (Thermal) (KCal.Mol)	158.453	713.706	1058.562
CV (Cal.Mol-Kelvi)	56.864	296.206	528.853
S (Cal.Mol-Kelvin)	134.286	282.642	506.696
Dipole moment (Debye)	5.3121	9.7738	2.8907
Point Group	C1	C1	C1
EHOMO (eV)	–0.30214	–0.24806	–0.30078
ELUMO (eV)	–0.07775	–0.22703	–0.1399
Eg (eV)	0.22439	0.02103	0.16088
I (eV)	0.30214	0.24806	0.30078
A (eV)	0.07775	0.22703	0.1399
χ (eV)	0.189945	0.237545	0.22034
η (eV)	0.112195	0.010515	0.08044
μ (eV)	–0.189945	–0.237545	–0.22034
ω (eV)	0.160787	2.683197	0.301776
S (eV)	4.456527	47.551117	6.215813

Table 2 — Electronic properties of the mechlorethamine calculated by using the B3LYP/6-31+G* level of theory

Property	Mechlorethamine	MC-SWCNT	MC-BNNT
HF (Hartree)	–1172.3022529	–4968.0516805	–8398.9072602
Zero-point correction (Hartree)	0.160937	1.009014	1.491755
Thermal correction to Energy (Hartree)	0.171126	1.065096	1.603840
Thermal correction to Enthalpy (Hartree)	0.172070	1.066040	1.604784
Thermal correction to Gibbs Free Energy (Hartree)	0.122885	0.937894	1.366664
Sum of electronic and zero-point Energies (Hartree)	–1172.141316	–4967.042667	–8397.415506
Sum of electronic and thermal Energies (Hartree)	–1172.131127	–4966.986585	–8397.303420
Sum of electronic and thermal Enthalpies (Hartree)	–1172.130183	–4966.985640	–8397.302476
Sum of electronic and thermal Free Energies (Hartree)	–1172.179368	–4967.113787	–8397.540596
E (Thermal) (KCal.Mol)	107.383	668.358	1006.425
CV (Cal.Mol-Kelvi)	34.145	274.149	506.952
S (Cal.Mol-Kelvin)	103.518	269.706	501.165
Dipole moment (Debye)	1.9530	2.6501	0.5689
Point Group	C1	C1	C1
EHOMO (eV)	–0.30002	–0.27704	–0.29653
ELUMO (eV)	–0.07561	–0.23501	–0.13987
Eg (eV)	0.22441	0.04203	0.15666
I (eV)	0.30002	0.27704	0.29653
A (eV)	0.07561	0.23501	0.13987
χ (eV)	0.187815	0.256025	0.2182
η (eV)	0.112205	0.021015	0.07833
μ (eV)	–0.187815	–0.256025	–0.2182
ω (eV)	0.157188	1.559572	0.303914
S (eV)	4.456129	23.792529	6.383250

the molecule[51]. In addition, the HOMO and LUMO can act as an electron donor and electron acceptor, respectively. An increased level of HOMO energy (EHOMO) for the molecule leads to the heightened ability for donating electrons to a suitable acceptor molecule, which has a low-energy empty molecular orbital. E_{HOMO} and E_{LUMO} are related to the ionization potential (I=-E_{HOMO}) and electron affinity (A=-E_{LUMO}), respectively[52,53]. Global hardness (η), electronegativity (χ), electronic chemical potential (μ), electrophilicity (ω), and chemical softness (S) parameters[54], are calculated by using the equations, which are given as follows:

$$(\eta = I - A/2) \quad (1) \quad \ldots(1)$$

$$(\chi = I + A/2) \quad (2) \quad \ldots(2)$$

$$(\mu = -(I + A)/2) \quad (3) \quad \ldots(3)$$

$$(\omega = \mu^2/2\eta) \quad (4) \quad \ldots(4)$$

$$(S = 1/2\eta) \quad (5) \quad \ldots(5)$$

The values of the parameters are shown in Table 1 and Table 2. The global hardness (η) parameter is related to the energy gap (Eg = E_{LUMO} – E_{HOMO}) and is defined as the charge transfer resistance of an atom or a group of atoms.

As shown in Table 1, the HOMO energy of the CP-BNNT compound has the lowest value (-0.30078 eV). A large energy gap between HOMO and LUMO indicates high molecular stability. The calculated HOMO-LUMO energy gap (ΔE) values for the structures CP-SWCNT and CP-BNNTs are 0.02103 and 0.16088 eV, respectively. The results demonstrate an increased energy gap for CP-BNNT compared to CP-SWCNT, indicating higher stability. Additionally, a molecule's reactivity is inversely related to its energy gap. The DOS plots illustrate the calculated energy gaps (ΔE) for CP (Fig. 4). Table 1 shows

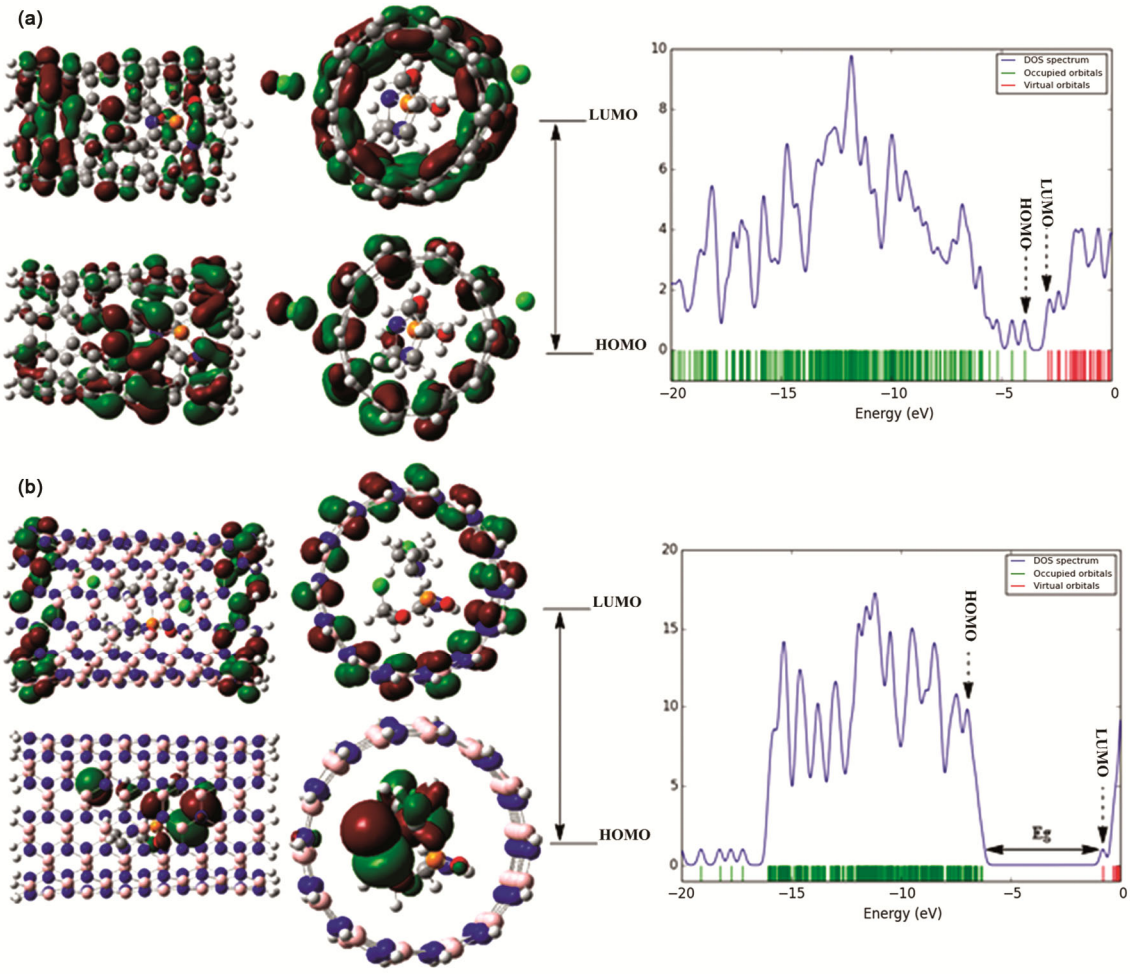

Fig. 4 — Calculated Frontier molecular orbitals and DOS plots [56, 57] of CP with SWCNT (a) and BNNT (b) (Eg: Energy gap between LUMO and HOMO)

specific quantum molecular descriptors for the title compounds, including ionization energy (I), electron affinity (A), electronegativity (χ), electronic chemical potential (μ=-(I + A)/2), chemical hardness (η), electrophilicity index (ω), HOMO-LUMO energy gap (Eg), and chemical softness (S).

The values of chemical hardness (η) for CP-SWCNTs and CP-BNNTs are 0.010515 eV and 0.08044 eV, respectively. Therefore, encapsulation of CP by boron nitride nanotube (BNNT) increases the chemical hardness (η = 0.08044 eV). As a result, CP-BNNTs exhibit lower softness and reactivity, leading to enhanced thermodynamic stability during delivery to diseased tissues. The electronic chemical potential (μ=-(I + A)/2) can be absorbed or released during chemical reactions and may undergo modification during phase transfer. The electronic chemical potential of CP-BNNT has the most negative value (-0.22034 eV). Based on the results, the Gibbs free energy values for CP-SWCNT and CP-BNNTs are 1.004015 and 1.447122 Hartree, respectively. The data indicates that the CP-BNNT compound possesses higher thermodynamic stability. Therefore, the thermodynamic stability of CP-BNNT is aligned with its energy gap and hardness values.

Electrophilicity (ω) is a measure of the ability of a system to stabilize energy upon receiving an additional electron from the environment. The index (ω=μ2/2η) incorporates information related to electron transfer (chemical potential) and stability (hardness). Moreover, it provides a more accurate description of global chemical reactivity. A higher electrophilicity index value increases the molecule's capacity to accept electrons. The electrophilicity indices for CP-SWCNT and CP-BNNTs are 2.683197 and 0.301776 eV, respectively. CP-SWCNTs have the highest electrophilicity index, indicating their high electron-accepting capacity.

The dipole moment (μD) is a vector quantity that indicates the difference in charges within a molecule. This property of the dipole moment leads to the creation of electron pairs in different atoms of the molecule, making the molecule asymmetric[55].

As shown in Table 1, all compounds exhibit high values of the dipole moment and belong to the C1 point group, indicating the asymmetry in the structures of the corresponding compounds. The dipole moment of CP-SWCNT (B3LYP/6-31+G (d) = 9.7738 Debye) is higher compared to CP-BNNT (2.8907 Debye).

In general, molecules with higher dipole moments tend to have lower stability, and this can be utilized in various applications, including drug design, catalysts, and novel chemical materials.

Therefore, considering the values of energy gap (Eg), chemical hardness (η), Gibbs free energy (G), dipole moment (μD), and electrophilicity (ω) for the structures of CP-SWCNT and CP-BNNTs, the results demonstrate that CP-BNNT is more stable than CP-SWCNT.

Table 2 indicates the specifics of the quantum molecular descriptors of the title compounds such as electron affinity, ionization potential, electronic chemical potential, global hardness, and electrophilicity.

As shown in Table 2, the calculated energy gaps between HOMO and LUMO for the compounds MC-SWCNT and MC-BNNTs are 0.04203 and 0.15666 eV, respectively. Based on the obtained results, it can be concluded that MC-BNNT is more stable.

Based on the obtained results, it can be concluded that MC-BNNT is more stable. Additionally, the Density of States (DOS) plots[56,57] illustrate the calculated energy gaps (ΔE) for MC (Fig. 5).

The values of chemical hardness (η) for the compounds MC-SWCNT and MC-BNNT are 0.021015 eV and 0.07833 eV, respectively. Therefore, encapsulation of MC by boron nitride nanotube (BNNT) increases the chemical hardness (η = 0.07833 eV). As a result, MC-BNNTs exhibit lower softness and reactivity, leading to enhanced thermodynamic stability during delivery to diseased tissues.

The electrophilicity index of MC-SWCNT and MC-BNNT are 1.559572 and 0.303914 eV, respectively. MC-SWCNTs have the highest electrophilicity index, indicating their high electron-accepting capacity. The dipole moment of MC-SWCNTs (2.6501 Debye) is higher compared to MC-BNNT (0.5689 Debye).

The Gibbs free energy values for MC-SWCNT and MC-BNNT are 0.937894 and 1.366664 Hartree, respectively. According to the results, the MC-BNNT combination has higher stability. The stability of the MC-BNNT combination is confirmed by the values of the HOMO-LUMO energy gap.

Therefore, considering the values of energy gap (Eg), chemical hardness (η), Gibbs free energy, dipole moment, and electrophilicity index for the structures of MC-SWCNT and MC-BNNTs, the results demonstrate that the MC-BNNT compound is more stable than CP-SWCNT. Hence, it can be said that the results for MC are generally similar to the results

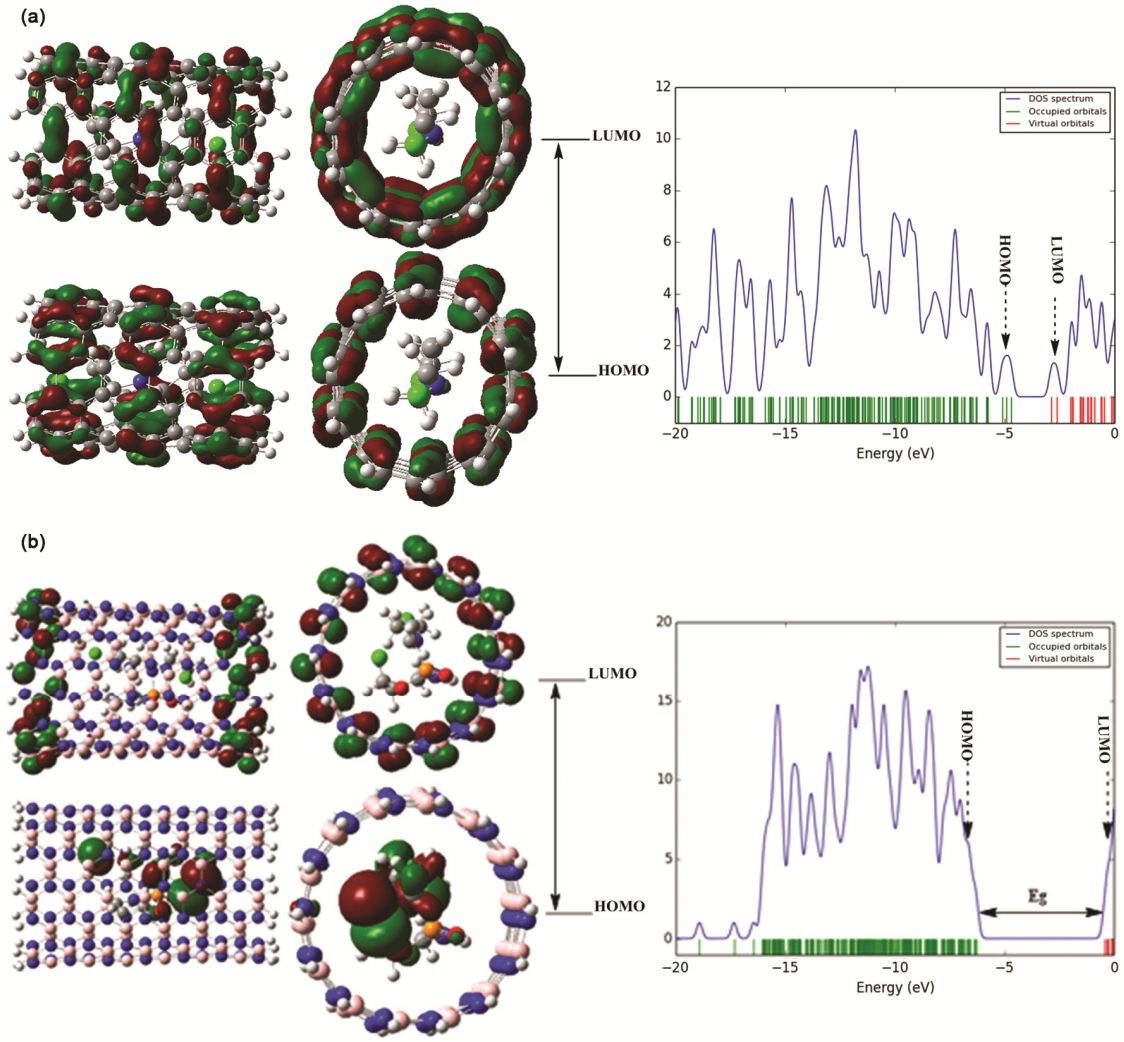

Fig. 5 — Calculated Frontier molecular orbitals and DOS plots[56,57] of MC with SWCNT (a) and BNNT (b) (Eg: Energy gap between LUMO and HOMO)

obtained for CP.

The total energy of a molecule is composed of translational, rotational, vibrational, and electronic energies. The thermodynamic statistical analysis of the title compounds is performed by placing the molecule at RT (25°C) and under 1 atmosphere pressure. Thermodynamic parameters such as zero-point vibrational energy, rotational constant, heat capacity (C), and entropy (S) of the title compounds are calculated using the B3LYP/6-31+G(d) level of theory, as shown in Table 1 and Table 2. The results of quantum mechanical calculations indicate that the stability of CP drug alongside BNNTs is higher, and BNNTs serve as a better adsorbent for it. Moreover, similar results were observed for MC.

Tables S1–S8 and S10-S17 indicate the results of the simulation and the molecular dynamic calculations of cyclophosphamide and mechlorethamine extracted in the form of the average of kinetic (E_{kin}) ((Figures S1 and S3), potential (E_{pot}) ((Figures S2 and S4), and total energies (E_{tot}) (Fig. 6, Fig. 7, Fig. 8 and Fig. 9) for boron nitride nanotube (BNNT) and Single-Walled carbon nanotube (SWCNT) in the CHARM, AMBER, OPLS, and MM+ force fields at Gas, Water, Methanol, Ethanol, DMSO and Chloroform solvents at the temperature range of 298-316 K (298, 300, 302, 304, 306, 308, 310, 312, 314, and 316) (Tables S1–S8 and S10–S17). When the calculations were conducted in the different force fields, it is worth noting that the energies obtained from various fields are different.

Investigating the kinetic energy diagrams shows that increasing the temperature gradually enhances the kinetic energy. The variations of the kinetic energy

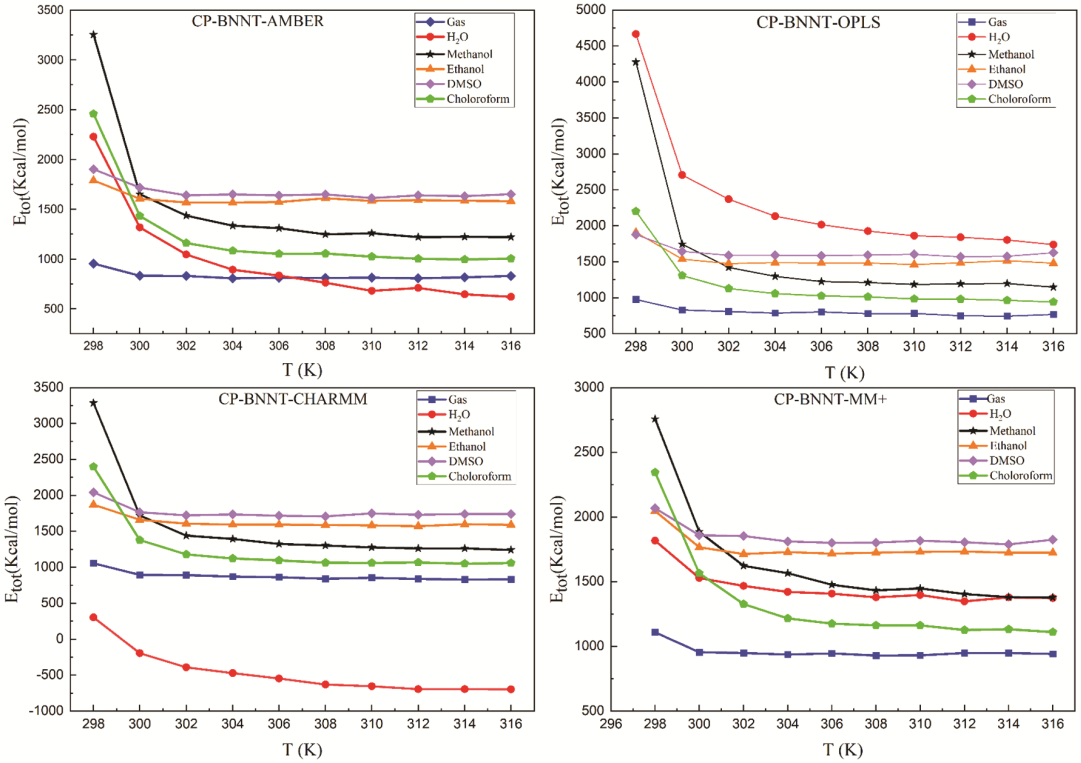

Fig. 6 — Total energies (E_{tot}) (kcal/mol) calculated *versus* temperature at different dielectric constants through Monte Carlo simulation in the AMBER, OPLS, CHARMM and MM+ force field for CP- BNNT

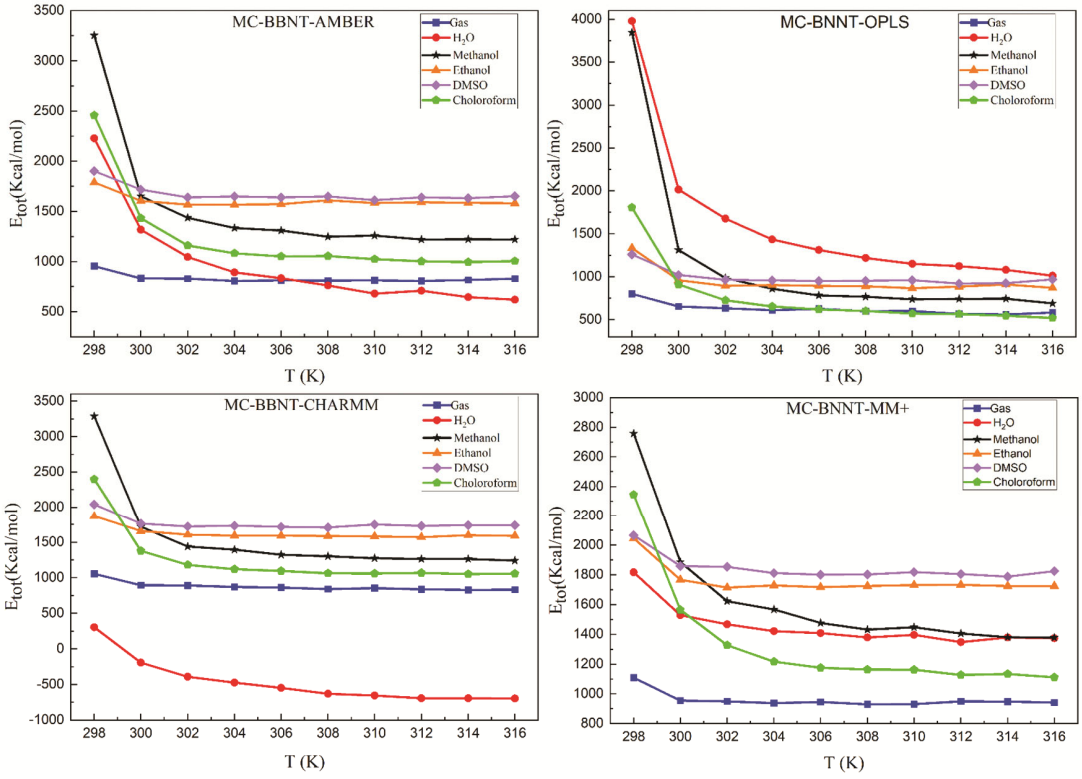

Fig. 7 — Total energies (E_{tot}) (Kcal/mol) calculated *versus* temperature at different dielectric constants through Monte Carlo simulation in the AMBER, OPLS, CHARMM and MM+ force field for MC-BNNT

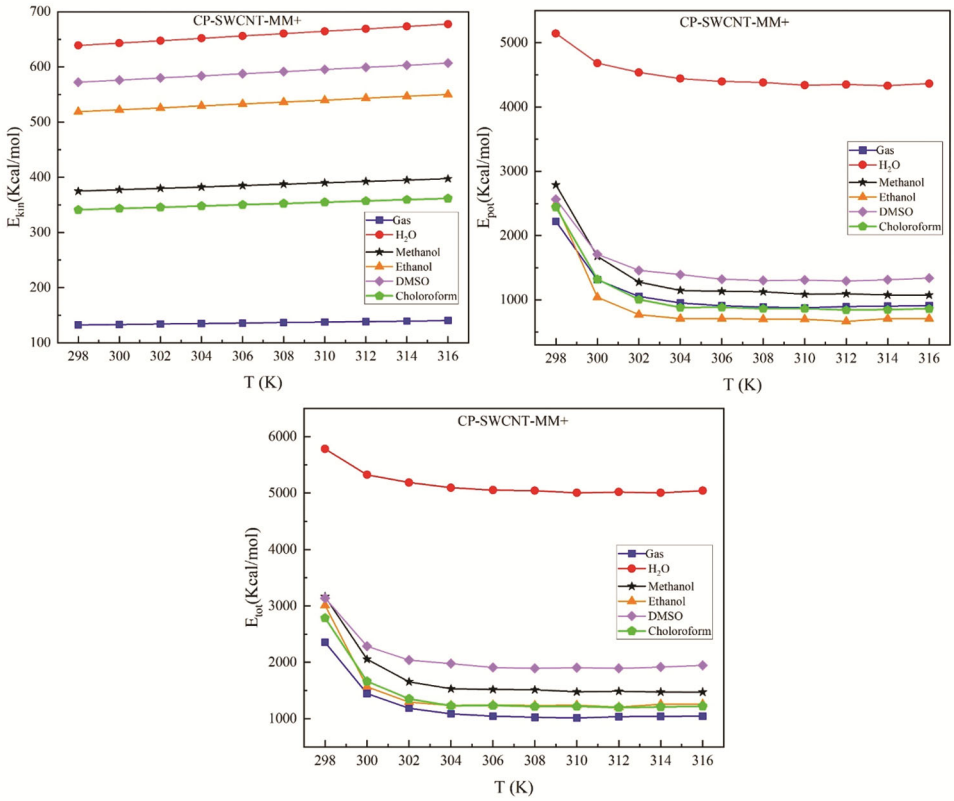

Fig. 8 — Kinetic (E_{kin}), Potential (E_{pot}) and Total (E_{tot}) energies (Kcal/mol) calculated *versus* temperature at different dielectric constants through Monte Carlo simulation in the MM+ force field for CP- SWCNT

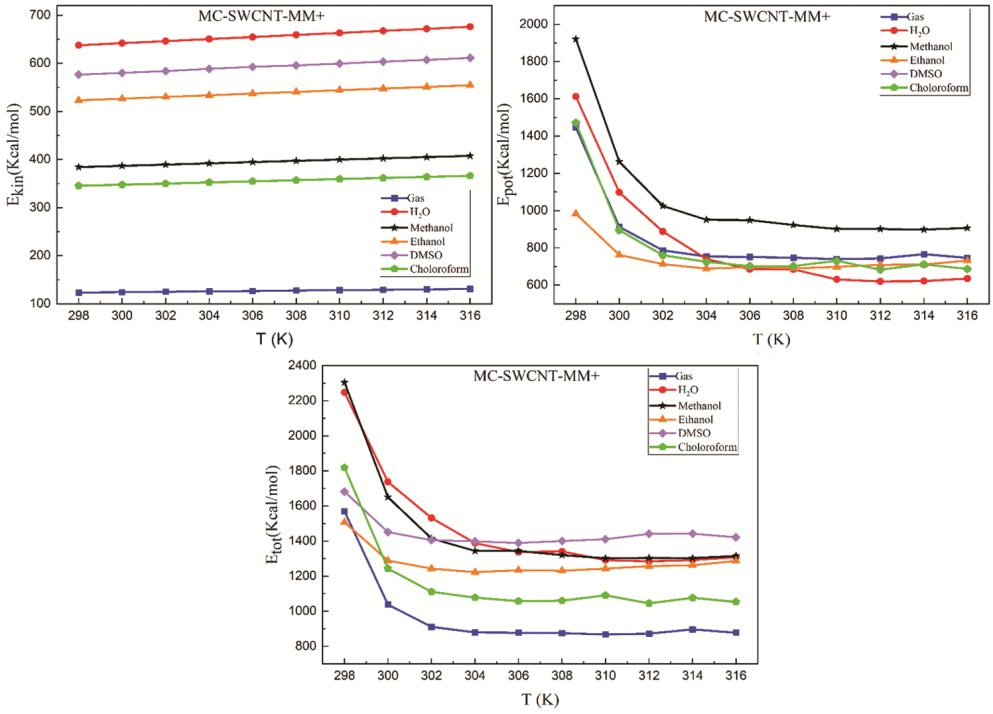

Fig. 9 — Kinetic (E_{kin}), Potntial (E_{pot}) and Total (E_{tot}) energies (Kcal/mol) calculated *versus* temperature at different dielectric constants through Monte Carlo simulation in the MM+ force field for MCe- SWCNT

versus temperature are linear with a positive slope. Therefore, the maximum and minimum kinetic energy are related to the temperature of 316 and 298 K, respectively. The amount of the kinetic energy is constant in different force fields (at the same temperature). The amount of the kinetic energy in water is higher than the other solvents. The order of the kinetic energy level (from low to high) is considered as Water- DMSO- Methanol- Ethanol- Chloroform. The general trend of variations of the potential and total energies is the same in all four fields and compositions. Initially, the level of the potential energy is high and then decreases with various slopes depending on the solvent type. In other words, the level of the potential energy decreases by increasing the temperature in all four fields and compositions. The detailed investigation is given in the following. The tables and diagrams indicate the total energy variations (E_{tot}) *versus* temperature in various solvents and force fields. The total energy is obtained from the following equation:

$$E_{tot}=E_{kin}+E_{pot} \quad \ldots(6)$$

Due to the linearity of the ascending trend of the kinetic energy, the variation trend of the total energy is a function of the potential energy variations. The variations of the potential and total energies *versus* temperature are of the nonlinear modes. Higher continuity and convergence indicate the more suitable force field and more realistic simulation model. Evaluating the plots of the total energy *versus* temperature shows that the continuity in the MM+ fields is higher than the others. Therefore, it is the more suitable field since the divergence of the results is obvious in the other fields.

The thermodynamic stability of each molecule is related to its energy level. The lower energy indicates the higher molecular stability. The details of the plots were investigated by focusing on the obtained results from this field. The total energy plot was evaluated in detail based on the similar trends of the potential energy variations for all of the compositions.

Cyclophosphamide-SWCNT

Investigating the kinetic energy of the compound indicated that increasing the temperature results in an elevated kinetic energy level and a declined potential energy level. The kinetic energy variations *versus* temperature are linear. However, the variations of the potential and total energy follow a nonlinear trend (Table S10-S13). Overall, the benzene ring in this molecule contributes significantly to its stability. Assuming the optimum force field as MM+, Table S9 shows minimum total energy and related temperature for each solvent and each compound. According to Table S9, minimum energy levels are related to the chloroform and ethanol solvents. The difference between the high level of energy of water and other solvents indicates the low water solubility of CP-SWCNT.

Cyclophosphamide-BNNT

Assuming the MM+ as the optimum field in the case of CP- BNNT, the temperature which gives the minimum total energy for each solvent is determined in Table S9**Error! Reference source not found.**. In general, the least amount of energy at various temperatures is related to the chloroform. Methanol and chloroform solvents are more quickly affected by the temperature enhancement, which reaches the minimum energy. The differentiation of the water-energy levels between the CP-BNNT and the CP-SWCNT, is related to the hydrogen bond formation between the nitrogen atom of the boron nitride nanotube and the hydrogen atom of the water. Moreover, the experimental data confirm the higher water solubility of BNNT compared to the carbon nanotubes.

Based on the data of MM+ plots, chloroform is a more suitable solvent for the CP- BNNT (Fig. 6) and ethanol and chloroform are more suitable solvents for CP- SWCNT (Fig. 8). The other solvents do not significantly differ from each other based on the energy levels for the two compositions.

Mechlorethamine-SWCNT

The variation trends are similar in all four fields. Initially, the potential energy is high and then decreases with various slopes depending on the type of solvent. In other words, the potential energy level decreases in all the solvents and the whole four fields (Tables S14-S17). The plot slope and the difference between the maximum and minimum energy points in the water, methanol, and chloroform plots are higher than the rest. The decline of the potential energy in all of the solvents is higher at 298-300 K and 302 K compared to the other temperatures. An increase in the temperature leads to a decrease in potential energy with a lower slope. Eventually, the descending trend stops in some solvents at the final temperatures of the

calculations, which turns into an ascending one. Based on the significant decline of the potential energy level at the first three temperatures of the plot in water, methanol, and chloroform, the dissolution and reaching the lower energy level occur faster in these solvents. However, chloroform is the most suitable solvent because it has both a lower energy level and a higher rate of reaching the lower energy. In other words, the solution stabilizes faster without further heating, and it is a more suitable solvent for MC- SWCNT. Moreover, the experimental data show that mechlorethamine relatively dissolves in water[58,59].

Mechlorethamine-BNNT

The slope and the difference between the maximum and minimum total energy points in the methanol and chloroform plots are higher than the other solvents (Tables S9). The decrease in the potential energy, in these solvents, is higher at 300 to 302 K than at the other temperatures. At higher temperatures, the potential energy decreases with a lower slope. The other solvents show fewer energy variations by increasing the temperature.

Based on the significant drop of the potential energy at the first three temperatures of the methanol and chloroform plots, the dissolution and reaching the lower energy occur faster in these solvents. In other words, the solution becomes stabilized and homogenous at a higher rate without any further heating. These solvents are more suitable for the MC-BNNT. Overall, the minimum total energy at different temperatures for this composition is related to the gas phase and chloroform. Methanol and chloroform total energy are rapidly affected by rising temperatures. In the case of water, it is less affected by the increasing temperature in comparison to MC- SWCNT. Moreover, the water has a trend similar to methanol for the MC- SWCNT. The visible difference in the energy level of the chloroform potential energy diagram illustrates that it is a better solvent for MC-SWCNT composition. Table S9, shows the minimum total energy and related temperature for each solvent and each compound. According to Table S9, chloroform is a suitable solvent for both MC-SWCNT (Fig. 9) and MC-BNNT (Tables S5–S8) (Fig. 7), but in the case of MC-BNNT, it needs more heat to reach the minimum energy.

Atom in molecule method

One of the calculation methods used to evaluate intramolecular bonds is AIM. In this calculation method, the density of electrons in the bonding space between two molecules is used as a means to study the nature and the strength of the interaction between two molecules. The points where the density of electron density is minimized are called critical bond points (BCP). Other parameters in the results are the second derivative of electron density: $\nabla^2 \rho(r)$, and total energy density (H). Intermolecular interaction can have a covalent or polar-covalent type when the electron density is high and the second derivative of the electron density is negative, and we have electrostatic bonds when the electron density is low and the second derivative of the density has a positive value. This means that the kinetic energy in the bonding space is greater than the potential energy. Another parameter that helps us determine the type of bonds is the V/G ratio. If V/G <1, the inter-molecular bond belongs to pure close-layer classification like Van der Waals, and if the 1<V/G <2, it indicates that the bond is a close-shell type like electrostatic and Hydrogen bond and for V/G >2 the bond is shared layer type like covalent bonds. Moreover $\nabla^2 \rho(r)$ and H have positive values that indicate the electrostatic types of bonds, on the other hand, the negative value of $\nabla^2 \rho(r)$and H, indicate the covalent bond. Positive $\nabla^2 \rho(r)$ and negative H is a sign of a weak covalent bond[60].

The AIM2000 program was used to perform the AIM calculations. The wave function of optimized complexes was used as an input for AIM[61].

AIM calculations related to MC-SWCNT, MC-BNNT, CP-SWCNT, and CP-BNNT compounds are shown in (Fig. 10). The AIM results for MC-SWCNT are reported in Table S18. The calculated values of ρ in BCPs in the range (0.0124–0.0345) a.u. are small, and V/G ≈1, which indicates that the interactions are partially covalent. The sign of $\nabla^2 \rho(r)$ is positive that indicate the weak interactions between MC and SWCNT.

For MC-BNNT the molecular graph is presented in Fig. 10 which demonstrates the positions of critical points and bond paths between medicine and nanotube. From the results reported in Table S19 the calculated values of ρ in the range of (0.22×10^{-2} – 0.73×10^{-2}) a.u. and V/G <1, which indicates that the most bonds between MC and BNNT are Van der Waals type. The value of $\nabla^2 \rho(r) > 0$ confirms the type of Intramolecular bonds. For H_9-N_{53} ($\nabla^2 \rho(r) > 0$ and negative H ($H < 0$) which indicate stronger hydrogen bond. The H9-N53 hydrogen bond has the

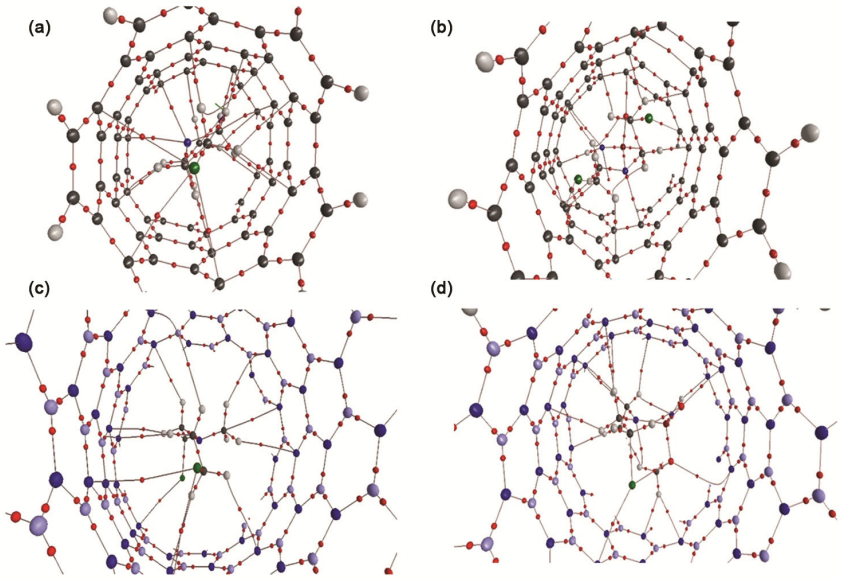

Fig. 10 — Molecular graph of medicine/nanotube Complexes obtained from AIM analysis. MC-SWCNT (a), CP-SWCNT (b), MC-BNNT (c) and CP-BNNT (d)

largest amount of ρ and the most amount $\nabla^2\rho(r)$ compared to other bonds, so it is stronger than other bonds Table S19.

Table S20 shows the AIM calculations related to CP-SWCNT. For most BCP, the $\nabla^2\rho(r)$ is positive and the $\frac{V}{G}$ ratio is about 1. The value of the electron density is low. All parameters indicate weak interaction Van der Waals between CP and SWCNT.

The AIM obtained results for CP-BNNT are listed in Table S21. The AIM parameters show weak hydrogen bond is dominant in this complex. The calculated values of ρ in BCPs in the range (0.0049–0.0244) a.u. are small and $\frac{V}{G} < 1$. For H_{21}-N_{34} Bond, because of the positive value of Laplacian and $\frac{V}{G} > 1$, there is a stronger hydrogen bond. For H26-N135 ($\nabla^2\rho(r) > 0$# and (H=-0.0009) which indicates a stronger hydrogen bond.

Therefore, based on the results of Molecular Mechanics, Quantum Mechanics calculations, and AIM parameters for CP-SWCNT, CP-BNNTs, MC-SWCNT, and MC-BNNT structures, it can be concluded that CP-BNNT and MC-BNNT compounds are more stable than CP-SWCNT and MC-SWCNT. So, BNNT is a better carrier for transporting CP and MC drugs and delivering these drugs to reach the target tissue.

Conclusion

The interaction of cyclophosphamide (CP) and mechlorethamine (MC) with Single wall carbon nanotubes (SWCNTs) and Boron nitride nanotubes (BNNTs) in the gas phase was evaluated by using the DFT calculations.

Through the DFT method, the effects of the different solvents were evaluated on the interaction of CP and MC molecules with SWNTs and BNNTs within the Onsager self-consistent reaction field (SCRF) model. Moreover, the effects of the temperature were investigated on the stability of the interaction between the compounds in various solvents. The theoretical calculations were resorted for investigating the Total Density of States (DOS), Frontier Molecular Orbitals (FMOs), and thermodynamic parameters of the title compounds. The molecular properties of the structures such as ionization potential (I), electron affinity (A), chemical hardness (η), electronic chemical potential (μ), and electrophilicity (ω) were analysed. The data showed that the CP- BNNT composition had more stability, which was confirmed further by the amounts of HOMO and LUMO energies and Gibbs free energy. In addition, the data indicated that the MC-BNNT composition had more stability, which was confirmed by the amounts of HOMO and LUMO energies.

The effect of different solvents and temperatures on the CP and MC (with SWNTs & BNNTs) was evaluated through quantum mechanics calculations and molecular mechanic simulation. Differences in the force fields were illustrated by comparing the energies calculated by using AMBER, OPLS,

CHARM (Bio+), and MM+ force fields.

Affecting the solvation free energies in the non-polar solvents shows significantly little variations across the solvents and force fields. However, this observation does not imply that the four force fields are essentially equivalent, and variations of the solvation free energy in more polar solvents only arise from differences in the atomic charges. The variability is significantly more pronounced when the non-polar molecules are considered as the solutes. The interaction parameters are largely correlated with the charges for polar molecules, the balance of which determines the geometry and strength of the favourable polar interactions (*e.g*. hydrogen bonds).

The chloroform solvent indicated the lowest amount of energy and proved to be the most stable solvent for the simulation, when CP connected to BNNTs was simulated in Water, Methanol, Ethanol, DMSO, and Chloroform solvents. Similar results were reported for OPLS and CHARMM force fields. However, the calculations related to the MM+ force field yielded a significant result. Water was the most stable and the most suitable solvent among the above-mentioned solvents for simulation in the MM+ field since it had the lowest amount of energy, which was related to the dielectric constant of the solvents positively. Water had the highest dielectric constant, which was considered the most suitable solvent for CP connected to BNNTs.

The results of MP connected to BNNTs were highly consistent with those related to MC connected to BNNTs. Methanol was the most stable solvent in the Amber, OPLS, and CHARMM force fields, and water was the most stable solvent in the MM+ field. The MM+ which is an exclusive force field for calculations related to the macromolecules had the lowest amount of energy and featured the most stable form of the connection for CP and MC connected to SWNTs and BNNTs. The CHARMM force field showed similar behaviour and put the compounds in a stable situation in some solvents and at certain temperatures. However, since the electrostatic reactions were calculated through the bipolar junctions by using the point charges in the MM+ field, the field managed to simulate the desired system in the most optimal way. Therefore, the MM+ force field was chosen as the most efficient field.

AIM analysis shows that hydrogen and van der Waals interactions between CP and MC drugs with BNNT are stronger than their interactions with SWCNT. The results of molecular electrostatic potential and transverse lines indicate greater interaction and electron resonance between drugs and BNNT.

Thus, the results of Monte Carlo, Molecular Mechanics, and Quantum Mechanics calculations are justified. In general, the results of the interaction of the drug CP and MC with both nanotubes show that BNNT is a better carrier in delivering these drugs to the patient's cells.

Delivering anti-cancer drugs through SWNTs and BNNTs is a significant breakthrough in the field of nanotechnology. Conventional management of cancers with chemotherapeutic agents can have adverse effects on healthy tissues. Therefore, developing the CNTs - based efficient drug delivery systems is necessary for delivering anti-cancer drugs. Although nano-technology is fairly developed, it is still far from clinical applications due to several challenges. However, SWCNTs- and BNNTs-based drug delivery systems are considered promising approaches for delivering anti-cancer drugs to the targeted organs or tissues. The results of this review paper indicated that the SWNTs- and BNNTs-based drug delivery systems might be highly effective and able to provide adequate scientific data for clinical support.

Supplementary Information

Supplementary information is available in the website http://nopr.niscpr.res.in/handle/123456789/58776.

Declaration of funding

This research did not receive any specific funding.

Conflict of interest

The authors declare no conflicts of interest.

Acknowledgements

The authors are thankful to Ahvaz Branch of Islamic Azad University and Zanjan Branch of Islamic Azad University for partial support of this work.

References

1 Vardanyan R, Hruby V, *Antiviral Drugs*, in *Synthesis of Best-Seller Drugs*, *Chap- 34,* (Academic Press, Boston) 2016, p. 687.

2 Emadi A, Jones R J & Brodsky R A, *Nat Rev Clin Oncol*, 6 (2009) 638.

3 Paci A, Rieutord A, Brion F & Prognon P, *J Chromat B: Biomed Sci App,* 764 (2001) 255.

4 Hossain M R, Hasan M M, Nishat M, Ahmed F, Ferdous T & Hossain M A, *J Mol Liq*, 323 (2021) 114627.

5 Gidwani B, Vyas A & Kaur C D, *Part Sci Tech*. 38 (2020) 23.
6 Xiang D, Huang P, Wang K, Zhou G, Liang Y & Dong D, *Chem Comm*, (2008) 6236. https://doi.org/10.1039/B815416C.
7 Steinbrecht S, Kiebist J, König R, Thiessen M, Schmidtke K-U, Kammerer S, Küpper J-H & Scheibner K, *AMB Express*, 10 (2020) 1.
8 Janelsins M C, Heckler C E, Thompson B D, Gross R A, Opanashuk L A & Cory-Slechta D A, *Neurotoxicology*, 56 (2016) 287.
9 Mauro F R, Carella A M, Molica S, Paoloni F, Liberati A M, Zaja F, Belsito V, Cortellezzi A, Rizzi R & Tosi P, *Leukemia Lymphoma*, 58 (2017) 1640.
10 Bhattacharjee A, Basu A, Biswas J, Sen T & Bhattacharya S, *Mol Cell Biochem*, 424 (2017) 13.
11 Kakaei A & Mirzaei M, *Lab-in-Silico*, 2 (2021) 9.
12 Felegari Z & Monajjemi M, *J Theor Comp Chem*, 14 (2015) 1550021.
13 Thirumaran R, Prendergast G C & Gilman P B, *Cytotoxic chemotherapy in clinical treatment of cancer*, in *Cancer immunotherapy*, (Elsevier) 2007, p. 101.
14 Ajazuddin, Alexander A, Amarji B & Kanaujia P, *Drug Dev. Ind. Pharm.*, 39 (2013) 1053.
15 Krasnov V P, Korolyova M A & Vodovozova E L , *Russian Chem Rev,* 82 (2013) 783.
16 Tabatabaei S N, Derbali R M, Yang C, Superstein R, Hamel P, Chain J L & Hardy P, *J Controlled Release*, 298 (2019) 177.
17 Guo R, Liu Q, Wang W, Tayebee R & Mollania F, *J Mol Liq*, 325 (2021) 114798.
18 Ritschel W A, Ye W, Buhse L & Reepmeyer J C, *Int J Pharm*, 362 (2008) 67.
19 Liu Z, Fan A C, Rakhra K, Sherlock S, Goodwin A, Chen X, Yang Q, Felsher D W & Dai H, *Angew Chem Int Ed*, 48 (2009) 7668.
20 Chegeni M, Rozbahani Z S, Ghasemian M & Mehri M, *Int J Biol Macromol*, 156 (2020) 504.
21 Sabahi A, Salahandish R, Ghaffarinejad A & Omidinia E, *Talanta*, 209 (2020) 120595.
22 Chopra N G, Benedict L X, Crespi V H, Cohen M L, Louie S G & Zettl A, *Nature*, 377 (1995) 135.
23 Zinlynezhad A, Nori-Shargh D, Najma N & Yahyaei H, *Phosphorus Sulfur Silicon*, 186 (2010) 44.
24 Xu H, Wang Q, Fan G & Chu X, *Theor Chem Acc*, 137 (2018) 1.
25 Merlo A, Mokkapati V, Pandit S & Mijakovic I, *Biomater Sci*, 6 (2018) 2298.
26 Gao Z, Zhi C, Bando Y, Golberg D & Serizawa T, *Nanobiomedicine*, 1 (2014) 7.
27 Juárez A R, Anota E C, Cocoletzi H H, Ramírez J S & Castro M, *Fuller Nanotub Carbon Nanostructures*, 25 (2017) 716.
28 Frisch M, Trucks G, Schlegel H, Scuseria G, Robb M, Cheeseman J, Scalmani G, Barone V, Mennucci B & Petersson G, See also: URL: http://www.gaussian.com. (2009).
29 Lee C, Yang W & Parr R G, *Phys Rev B: Condens Matter*, 37 (1988) 785.
30 Johnson B, Seminario J & Politzer P, *Modern Density Function Theory: A Tool for Chemistry*, (Elsevier, Amsterdam) 1995.
31 Becke A, *J Chem Phys*, 98 (1993) 5648.
32 Tomasi J, Mennucci B & Cammi R, *Chem Rev*, 105 (2005) 2999.
33 Shahab S, Sheikhi M, Filippovich L, Dikusar E, Yahyaei H, Kumar R & Khaleghian M, *J Mol Struct*, 1157 (2018) 536.
34 Yahyaei H, Sharifi S, Shahab S, Sheikhi M & Ahmadianarog M, *Lett Org Chem*, 18 (2021) 115.
35 Shahab S, Sheikhi M, Filippovich L, Kumar R, Dikusar E, Yahyaei H & Khaleghian M, *J Mol Struct*, 1148 (2017) 134.
36 Frisch A, Nielson A & Holder A, *Gaussian Inc Pittsburgh, PA*. 556 (2000).
37 Szczepanska A, Espartero J L, Moreno-Vargas A J, Carmona A T, Robina I, Remmert S & Parish C, *J Org Chem*, 72 (2007) 6776.
38 Metropolis N, Rosenbluth A W, Rosenbluth M N, Teller A H & Teller E, *J Chem Phy,* 21 (1953) 1087.
39 Cornell W, Cieplak P, Bayly C I, Gould I R & Merz J, *J Am Chem Soc*, 117 (1995) 5179.
40 Jorgensen W L, Tirado-Rives J, *J Am Chem Soc*, 110 (1988) 1657.
41 MacKerell A D, Bashford D, Bellott M, Dunbrack R L, Evanseck J D, Field M J, Fischer S, Gao J, Guo H & Ha S, *J Phys Chem B*, 102 (1998) 3586.
42 Neria E, Fischer S & Karplus M, *J Chem Phy,* 105 (1996) 1902.
43 HyperChem R, *7.0 for windows, Hypercube*. 2002, Inc.
44 Yahyaei H, Monajjemi M, Aghaie H & Zare K, *J Comput Theor Nanosci*, 10 (2013) 2332.
45 Kastner M, *Commun Nonlinear Sci Numer Simul*, 15 (2010) 1589.
46 Hastings W K, *Biometrika*, 57 (1970) 97.
47 Liu J S, Liang F & Wong W H, *J Am Stat Assoc*, 95 (2000) 121.
48 Champion J A & Mitragotri S, *Proc Natl Acad Sci U S A*, 103 (2006) 4930.
49 Kinnings S L, Liu N, Buchmeier N, Tonge P J, Xie L & Bourne P E, *PLoS Comp Biol*, 5 (2009) e1000423.
50 Collins I & Workman P, *Nat Chem Biol*, 2 (2006) 689.
51 Scheinfeld N, *Dermatol Online J*, 12 (2006). https://doi.org/10.5070/D30nq2c0bx.
52 Sawaya M R & Kraut J, *Biochem*, 36 (1997) 586.
53 Cronstein B N, *Pharmacol Rev*, 57 (2005) 163.
54 Meyer L M, Miller F R, Rowen M J, Bock G & Rutzky J, *Acta Haematol*, 4 (1950) 157.
55 Yadav V K, *Steric and Stereoelectronic Control of Molecular Structures and Organic Reactions*, in *Steric and Stereoelectronic Effects in Organic Chemistry*, (Springer) 2021, p. 1-48.
56 O'boyle N M, Tenderholt A L & Langner K M, *J Comp Chem*, 29 (2008) 839.
57 O'Boyle N, *GaussSum, Version 2.0. 5,* . 2007.
58 Anderson D, McGregor D B, Purchase I F H, Hodge M C E & Cuthbert J A, *Mut Res Funda Mole Mechs Mut*, 43 (1977) 231.
59 Reepmeyer J C, *J Chromatogr A*, 1085 (2005) 262.
60 Bououden W, Benguerba Y, Darwish A S, Attoui A, Lemaoui T, Balsamo M, Erto A & Alnashef I M, *J Mol Liq*, 338 (2021) 116666.
61 Biegler-König F, Schönbohm J, Derdau R, Bayles D & Bader R, *University of Applied Sciences, Bielefeld, Germany*. (2000).